Evidence for universal intermittent crystal plasticity from acoustic emission and high-resolution extensometry experiments

Jérôme Weiss,[1,*] Thiebaud Richeton,[1,2] François Louchet,[1] Frantisek Chmelik,[3] Patrick Dobron,[3] Denis Entemeyer,[2] Mikhail Lebyodkin,[2] Tatiana Lebedkina,[4] Claude Fressengeas,[2] and Russell J. McDonald[5]

[1]*Laboratoire de Glaciologie et Géophysique de l'Environnement/CNRS, 54 rue Molière, Boîte Postale 96, 38402 St. Martin d'Hères Cedex, France*

[2]*Laboratoire de Physique et Mécanique des Matériaux, Université Paul Verlaine-Metz/CNRS, Ile du Saulcy, 57045 Metz Cedex, France*

[3]*Department of Physics of Materials, Charles University, Ke Karlovu 5, CZ-121 16 Prague 2, Czech Republic*

[4]*Institute of Solid State Physics, Russian Academy of Science, 142432 Chernogolovka, Russia*

[5]*Department of Mechanical Sciences and Engineering, University of Illinois at Urbana-Champaign, 1206 West Green Street, Urbana, Illinois 61801, USA*

(Received 4 October 2007; revised manuscript received 5 November 2007; published 21 December 2007)

Plasticity, a key property in the mechanical behavior and processing of crystalline solids, has been traditionally viewed as a smooth and homogeneous flow. However, using two experimental methods, acoustic emission and high-resolution extensometry, to probe the collective dislocation dynamics in various single crystals, we show that its intermittent critical-like character appears as a rule rather than an exception. Such intermittent, apparently scale-free plastic activity is observed in single-slip as well as multislip conditions and is not significantly influenced by forest hardening. Strain bursts resulting from dislocation avalanches are limited in size by a nontrivial finite size effect resulting from the lamellar character of avalanches. This cutoff explains why strain curves of macroscopic samples are smooth, whereas fluctuations of plastic activity are outstanding in submillimetric structures.

DOI: 10.1103/PhysRevB.76.224110 PACS number(s): 62.20.Fe

I. INTRODUCTION

As suggested by its very name and by smooth macroscopic stress-strain or creep curves, the classical view of plastic "flow" in crystalline materials is that of a smooth and homogeneous process. Exceptions are "exotic" cases such as the Portevin—Le Chatelier effect, which involves complex interactions between dislocations and solutes and is characterized by jerky flow with large stress drops on stress-strain curves.[1] Yet, intermittency of plastic activity has been known for a long period of time. For example, it was described in Zn single crystals as early as 1932.[2] However, these observations remained marginal, as the observed fluctuations were seen as sufficiently small and independent of one another to add at random to a smooth overall response. A fundamentally different picture emerged during the last few years, that of a scale-free intermittent plastic activity characterized by power law distributions of dislocation avalanche sizes,[3,4] time correlations and aftershock triggering,[5] as well as fractal patterns and complex space-time coupling.[6] Experimental evidence came from acoustic emission (AE) experiments on deformed ice single crystals that showed power law distributions of AE amplitude and energy.[3,4] The maximum AE amplitude A_0 of an event is a measure of the initial surface-sweeping rate of dislocations. Assuming an exponential decay for AE amplitude, A_0 can also be considered as a proxy of the strain increment ε carried by the avalanche.[7] These findings are supported by different modeling approaches including two-dimensional[4] and three-dimensional (3D)[8] discrete dislocation dynamics and phase-field[9] or continuum[10] models. Independent experimental support was obtained from compression tests on Ni micron-size single crystals that showed staircaselike stress-strain curves with power law distribution of step size.[11]

All of these findings argue for a renewed viewpoint on crystalline plasticity, reminiscent of the concept of crackling noise[12] describing out-of-equilibrium physical systems with bursts of activity (avalanches) in close vicinity to criticality. We conjecture a rather universal character for such intermittent plasticity: fluctuations would be the rule, not the exception. We note, however, that (i) the existence of an internal length scale in polycrystals, the average grain size, limits the amplitude of fluctuations and therefore breaks down the scale invariance,[13] and that (ii) there are still doubts on whether this critical dynamics develops in materials with low dislocation mobility (because of, e.g., high lattice friction), when obstacles to dislocation motion (such as Peierls barriers, microparticles) either hinder or slow down free rearrangements of the dislocation population.[14]

In single crystals with high dislocation mobility, two fundamental questions remain unanswered. (1) So far, intermittency and scaling in plasticity have been observed only under single-slip conditions. Does the critical dynamics we envision extend to multislip plasticity, or does multislip break down scale invariance by virtue of forest hardening?[10,15] (2) If a scale-free, critical dynamics is indeed existent, why are the largest strain bursts not detectable? In other words, why are macroscopic strain curves smooth if a statistical offset of fluctuations cannot be called for an explanation, or why is intermittence not seen at all length scales?

II. ACOUSTIC EMISSION IN hcp AND fcc SINGLE CRYSTALS

The AE source model, which allows to interpret the AE wave characteristics in terms of a source mechanism, has been detailed elsewhere.[7] This model was initially inspired

by the work of Rouby *et al.*[16] We recall here the points needed for an interpretation of our results. Making a low frequency assumption ($<10^6$ Hz) and considering the case of an acoustic transducer responding to surface velocity, one can relate the amplitude of the acoustic wave A resulting from a dislocation avalanche to the total dislocation length L involved in the avalanche and the dislocation velocity v (averaged over L),

$$A(t) \sim bLv, \tag{1}$$

where b is the magnitude of the Burgers vector. The term Lv accounts for the surface S swept by time unit by dislocations during the avalanche,

$$Lv = \frac{dS}{dt}. \tag{2}$$

When multiplied by b and normalized by a volume, this term represents a strain rate $d\varepsilon/dt$. Combining relations (1) and (2) gives therefore

$$A(t) \sim V\frac{d\varepsilon}{dt}, \tag{3}$$

where V is the volume considered (e.g., the sample volume). Only the maximum amplitude of the acoustic burst, which roughly corresponds to the initial amplitude A_0, is generally recorded and analyzed. It corresponds to the initial sweeping rate $(dS/dt)_0$. To estimate the "strained volume" $S \times b$, and consequently, the strain increment ε carried by the avalanche, after normalization by V, one has to know how this initial sweeping rate decays with time. The shape of the acoustic bursts argues for an exponential decay,[7] that is, for the equivalent strain rate,

$$\frac{d\varepsilon}{dt} = \left(\frac{d\varepsilon}{dt}\right)_0 \exp[-\alpha(t-t_0)], \tag{4}$$

where the decay coefficient α might be interpreted as a drag coefficient. Note that this decay corresponds to the source of the AE signal, i.e., to the sweeping rate dS/dt, and not to the acoustic wave itself, whose damping is negligible. Such an exponential decay implies a $\Delta t \sim (1/\alpha)\log(A_0)$ relationship,[7] where the duration Δt of the acoustic burst is defined as the time interval over which the envelope of the signal remains above the detection threshold. In our experiments, such relationship is observed up to $A_0 \approx 0.2$ V, i.e., for more than 98% of the events. Then, by integrating relation (4) over time and using relation (3), we obtain a model of AE source which relates directly the value of the maximum amplitude of the acoustic wave A_0 to the "strained volume" $S \times b$ or the strain increment ε,

$$\varepsilon = \frac{Sb}{V} \sim \frac{A_0}{\alpha V}. \tag{5}$$

The exponential decay [Eq. (4)] and the associated relationship $\Delta t \sim (1/\alpha)\log(A_0)$ may seem to be rather unusual in the context of criticality. Indeed, they can be seen as inconsistent with the power law scaling $\Delta t \sim A_0^k$ generally reported for avalanche processes in models of critical phenomena, such as sandpile models of self-organized criticality.[17] As a matter of fact, such a power law scaling reasonably fits our AE data for large amplitudes ($A_0 > 0.2$ V), with $k \approx 0.6$. In the present case, we interpret this change of regime by the fact that for large events, the acoustic signal remains above the threshold for the period of time between the mainshock and several subsequent aftershocks. Hence, the latter are counted with the mainshock. In other words, the sequence of aftershocks obeys a power law, Omori-like decay,[18] $1/(t+c)^p$, where c is a (small) time constant, and the duration scales as $\Delta t \sim A_0^{1/p}$, i.e., $p = 1/k \approx 5/3$. This might suggest to consider such a cascade of triggered aftershocks to belong to one single "avalanche." An analysis of this problem is left for future work. Another expression of this Omori-like decay of aftershock triggering is given by the average number of aftershocks triggered by a "mainshock" of amplitude A, N_A, that scales as $N_A \sim A^{k'}$, again with $k' = 0.6$.[5] We can finally note that a power law, Omori-like decay for the sweeping rate with $p > 1$ would also lead to A_0 being proportional to the strain increment ε.

AE was recorded during constant crosshead speed tensile tests on Cd, Zn-0.08%Al, and Cu single crystals at room temperature. The initial strain rates ranged from 1.1×10^{-3} to 2×10^{-3} s^{-1} for Zn and Cd and from 2.9×10^{-4} to 3.8×10^{-2} s^{-1} for Cu. A miniaturized piezoelectric transducer (frequency band of 100–600 kHz) was fastened to the surface of each specimen. Whereas ice single crystals exhibit no strain-hardening during deformation, specimens of hexagonal metals (Cd, Zn) with orientations favorable to basal glide exhibit a typical easy basal glide stage I, characterized by a low stress plateau, followed by stage II hardening with a sharp increase in the hardening rate, due to the activation of nonbasal slip systems. At larger strains, stage III is observed with serrations characteristic of twinning. Twinning, another significant source of AE, is an important deformation mechanism in hcp metals. It is assumed to proceed through motion of partial dislocations.[19] As a consequence, the proportionality between A_0 and ε differs from that of avalanches of perfect dislocations.[20] Slip avalanches and twinning events can also be discriminated from their AE wave forms.[20,21] Despite these differences and the strong increase in the proportion of twinning events vs slip avalanches from stage I to stage III, plastic deformation of hcp metals was characterized by intermittent AE activity showing power law distribution of AE amplitudes, $P(A_0) \sim A_0^{-\tau}$ with a single exponent $\tau = 2.0 \pm 0.1$, regardless of the material and of the stage of deformation, and identical to the one obtained in ice testing. This distribution did not change as the hardening coefficient θ jumped in the transition from stage I to stage II (Fig. 1). A time clustering of AE events was systematically revealed by an aftershock analysis. Furthermore, it was verified that slip avalanches can trigger twinning, and vice versa,[20] illustrating the mutual interactions between these two deformation mechanisms and their participation in the same global dynamics.

These observations on hcp crystals make a compelling argument in favor of a generic scale-free critical framework for crystal plasticity, irrespective of the material, the loading mode (creep vs displacement controlled), the nature of dis-

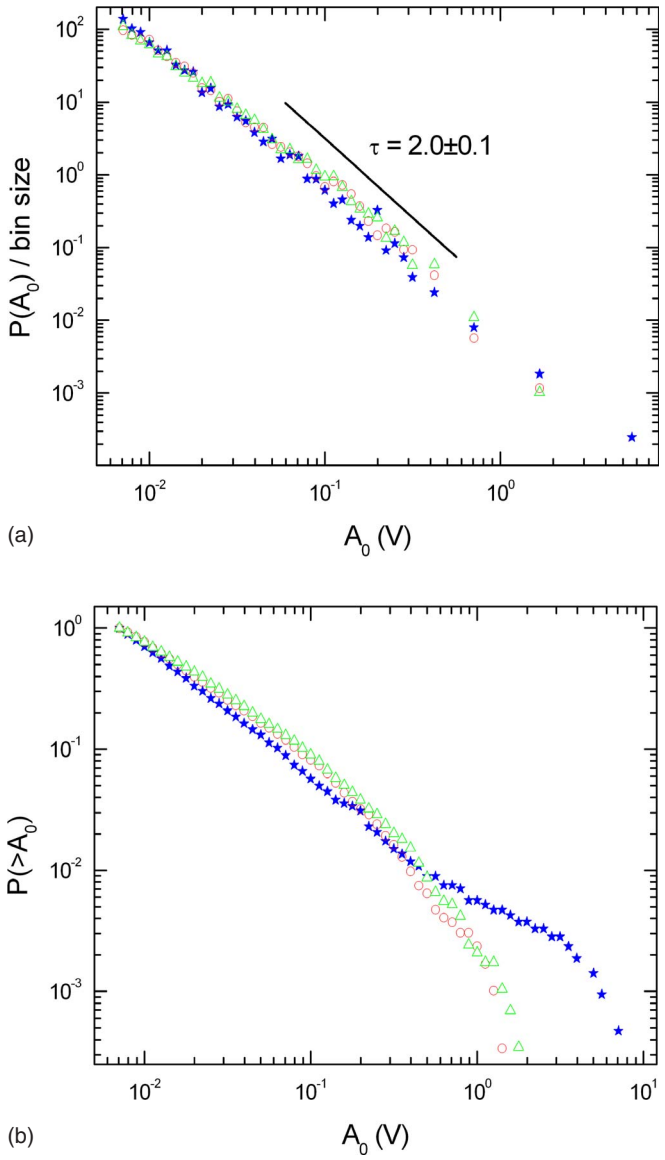

FIG. 1. (Color online) (a) AE amplitude probability density functions and (b) rank ordering statistics obtained during the plastic deformation of ice and Cd single crystals. This reveals truncated power law distributions of dislocation avalanche sizes, $P(A_0) \sim A_0^{-\tau} f(A_0/A_c)$, where the exponent $\tau=2.0\pm0.1$ is independent of the material and/or the sample size and $f(x)$ is a cutoff function. Truncation of the distributions is not apparent on the pdf's, but clearly detectable on rank ordering statistics. For the Cd sample, the cutoff A_c is not sensitive to the jump of the strain-hardening coefficient θ from stage I to stage II. Stars: compression creep loading of an ice single crystal (sample length of 68.2 mm, sample diameter of 37.4 mm, $T=-10$ °C, applied stress of 0.76 MPa, Schmid's factor $m=0.25$, and negligible strain hardening). Open circles: tensile test under constant crosshead velocity of a Cd single crystal, stage I (initial sample length of 25 mm, initial sample diameter of 3.6 mm, $T=20$ °C, initial strain rate of 1.3×10^{-3} s^{-1}, Schmid's factor $m=0.46$, and $\theta\approx0.8$ MPa$\approx E/62\,500$, where E is the elastic modulus). Open triangles: same test, stage II (strain hardening coefficient $\theta\approx4.7$ MPa$\approx E/10\,600$). The three different distributions have been plotted for the same number of events (3539). For the records containing more than 3539 events, we checked that the normalized rank ordering statistics were not affected by this undersampling.

locations (i.e., those related to slip or to twinning), and the forest-hardening level. However, plasticity in hcp metals remains anisotropic, with only a small contribution of nonbasal planes to overall plastic strain, even during stage II. In contrast, Cu represents the true emblematic multislip situation where different slip systems can contribute significantly to macroscopic strain, whereas twinning is absent. For the tests on Cu single crystals, strong strain hardening occurred immediately, without detectable stage I, indicating that multislip was activated from the early stages of deformation. Intermittent AE activity was detected during each test, in agreement with previous work,[22] although the number of events per unit strain was strongly reduced as compared to hcp metals (few tens to few hundreds per test compared to several thousand). Again, AE amplitudes were distributed according to a power law with exponent $\tau=2.0$ [Fig. 2(a)], which supports further the ubiquitous character of the underlying critical dynamics. Time clustering of avalanches and aftershock triggering was evidenced by means of a correlation integral analysis, as the number of events was too limited for a detailed aftershock analysis [Fig. 2(b)].

III. HIGH-RESOLUTION EXTENSOMETRY

Independent experimental support for the intermittent, self-organized character of collective dislocation dynamics in multislip was obtained from high resolution extensometry. As to the present purpose, significant differences with AE measurements must be mentioned. They reside in the much lower recording frequency, the direct measurement of plastic displacements, and the point wise character of these measurements. Flat samples extracted from a copper single crystal were oriented for multislip and loaded in tension with constant crosshead velocity. Several tests were made with overall strain rate ranging from 5×10^{-5} to 5×10^{-3} s^{-1}. Each time, the sample was clamped and no rotation of cross sections was observed before the onset of necking. On one side of the sample, the surface was painted in black, and strips of white paint normal to the longitudinal axis were superimposed, resulting in a network of black and white strips approximately 1 mm wide. The strips are neatly tied with the material underneath, and their displacement reflects perfectly the material displacement. A high resolution charge coupled device camera with recording frequency of 10^3 Hz and pixel size of 1.3 μm with the lens in use was mounted to capture the longitudinal displacement of points set at the intersection of the symmetry axis (to avoid any cross-section rotation effect) with the transitions between black and white strips. We used 15–20 such points, defining as many elementary extensometers with gauge length about 1 mm. From the onset of necking onward, strain localization occurs in a section of the sample, and the data are discarded as to the present purpose.

These local displacement records (Fig. 3) were derived to obtain Lagrangian velocities $v(t)$, which exhibit a jerky character (Figs. 4 and 5). The self-similar character of this velocity signal is the subject of the investigation. It is intuitively shown by the successive close-ups of the velocity signal in Fig. 4. The probability density function for bursts in the ve-

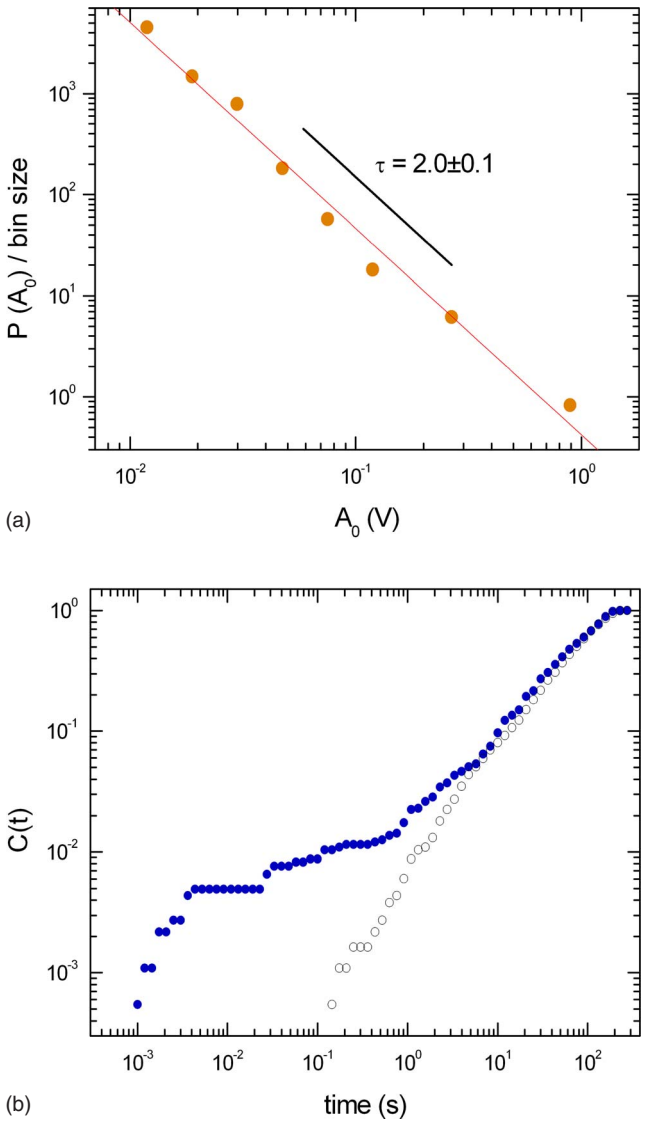

FIG. 2. (Color online) AE recorded during the tensile plastic deformation of Cu single crystals (initial sample length of 20–60 mm, initial sample diameter of 4 mm, and Schmid's factor $m \approx 0.3$). (a) AE amplitude probability density function obtained by collecting data recorded during six different tests under constant crosshead speed ($T=20$ °C, initial strain rates varying from 2.9×10^{-4} to 3.8×10^{-2} s^{-1}, and maximum hardening coefficient θ varying from $E/1000$ to $E/3300$). (b) Correlation integral analysis calculated for one of these tests (initial strain rate of 5.1×10^{-3} s^{-1}). The correlation integral $C(t)$ is the probability for two events to be separated by less than a time t and is defined as $C(t) = [2/N(N-1)]n(\Delta t < t)$, where N is the number of considered events and $n(\Delta t < t)$ the number of pairs of events separated by less than t. The AE dataset (closed circles) is compared to a similar analysis performed on the same number of events ($N=61$) randomly distributed in time (Poisson process, open circles). The random dataset follows the expected scaling $C(t) \sim t$, whereas a time clustering of the AE events is observed below 5 s.

locity of a sample cross section may be drawn in several different ways, depending on how the bursts are defined. However, all the plots thus obtained show a trend similar to that displayed in Fig. 5 for the peak velocity values: they are

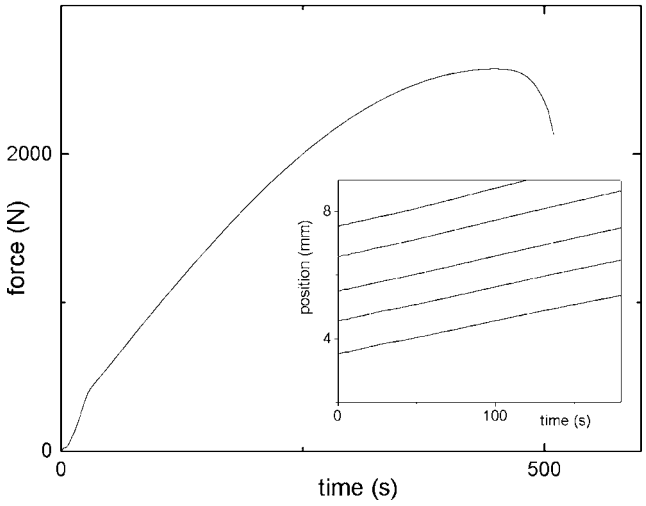

FIG. 3. Cu single crystal oriented for multislip loaded under uniaxial tension (thickness of 2 mm, width of 10 mm, length of 35 mm, Schmid's factor $m=0.3$, and $T=20$ °C. The applied strain rate is 5×10^{-4} s^{-1}. Macroscopic force vs time curve (main graph) and displacement vs time in five different locations along the sample (inset). The initial stage II hardening rate is $\theta \approx 7E/1000$. The displacements were recorded at intervals of 1 mm in 20 sections of the samples.

consistent with power law scaling, again with scaling exponent $\tau=2.0$, although the available scale range is limited by the resolution. The robustness of this behavior is in itself an indication of self-similarity.

In order to gain insights into correlations in time, these records were also analyzed by means of a multifractal analysis, in the spirit of previous work on jerky flow.[23] We defined the measure μ_i of jerk intensity during the ith time interval, of duration δt, as the sum of the absolute values of the measured velocities over this interval, normalized by a similar sum over the entire record. In a standard way,[24] the strength of the jerk singularity, i.e., the relation between its measure μ_i and duration δt, was sought through the qth moment $Z_q(\delta t) = \Sigma_{i=1}^{n} \mu_i^q$. Calculated over all n intervals, the latter was observed to scale as $Z_q \sim \delta t^{(q-1)D(q)}$, where $D(q)$ is the generalized fractal dimension. The spectrum $D(q)$ characterizes the scaling properties of the dataset as q varies (Fig. 6). A more detailed description of the application of multifractal analysis to deformation curves, fully applicable to the present data, can be found elsewhere.[25]

For purely random fluctuations, as those expected from smooth and homogeneous plastic flow, $D(q)$ would be uniformly independent of q and equal to 1. Instead, the wide range of the multifractal spectrum in Fig. 6 is the fingerprint of long-range time correlations involving an extended set of scaling indices. The scaling range extends over two orders of magnitude and testifies to correlations between avalanches (e.g., from 0.1 to 20 s for the data in Fig. 6), in agreement with aftershock triggering revealed by AE.[5] This spectrum was found to be very robust and fairly insensitive to the location along the sample axis. It is also weakly dependent on the applied strain rate, another possible hint at the universality of the underlying dynamics.

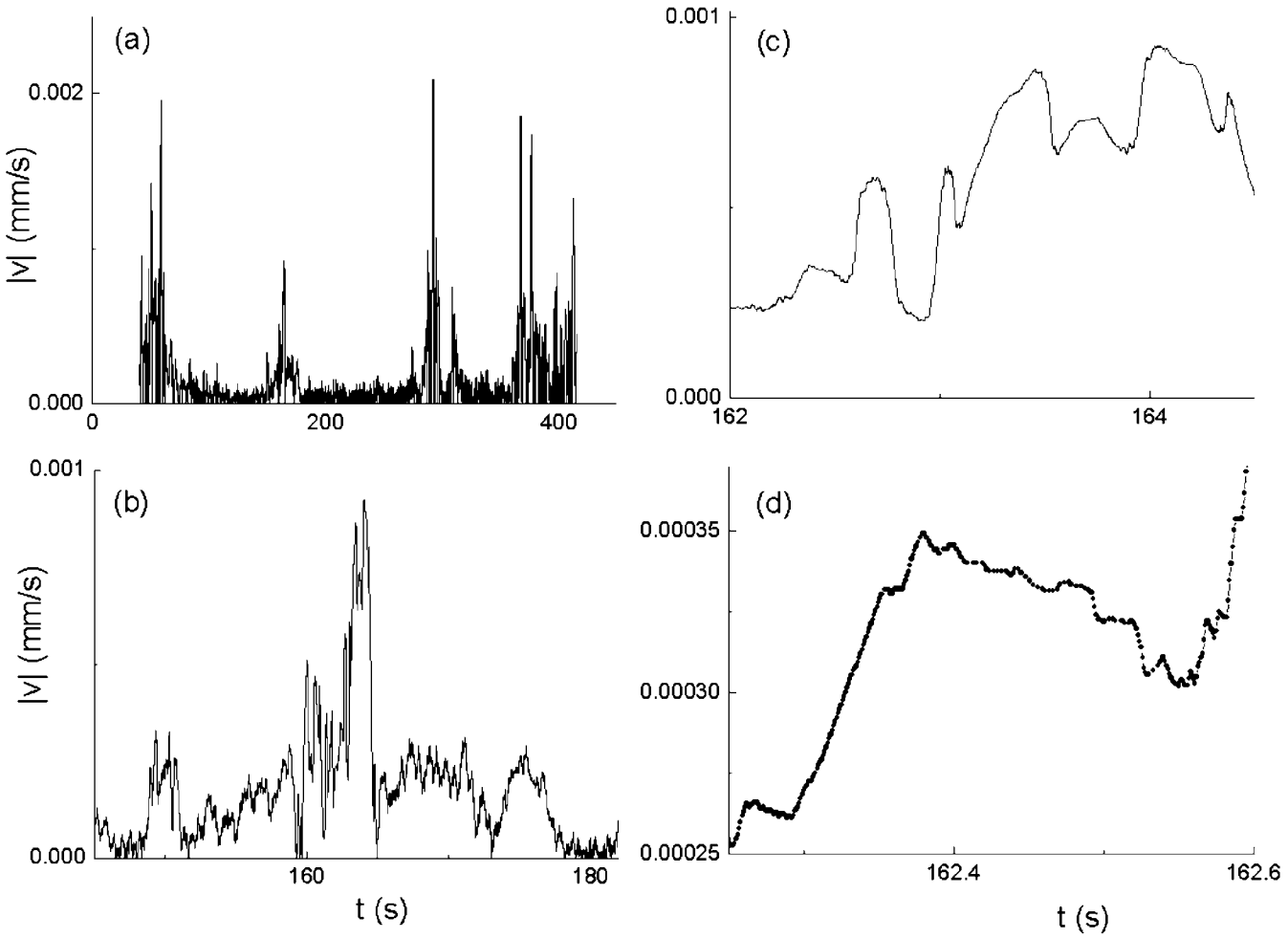

FIG. 4. Velocity signals from high-resolution extensometry derived from the displacement vs time record shown on Fig. 3. The long-term trend of the displacement-time curve on the time scale of the experiment was subtracted from the measured signal before derivation. Sequence of close-ups of the velocity signal shown in Fig. 5, suggesting scale invariance.

IV. DISCUSSION AND CONCLUSION

The above results, based on different experimental methods and gathered from various materials in single-slip or multislip, with distinct crystallographic structures, hardening coefficients and loading conditions, support the notion of the universality of time-correlated intermittency and power law scaling in avalanche statistics. They are consistent with the notion of an ubiquitous close-to-criticality character of crystal plasticity.

A natural conjecture in tracking the physical factors promoting correlated behavior in intermittent plasticity is to attribute its driving force to the long-range elastic stress and lattice curvature fields associated with "polar" (or "excess" or "geometrically necessary") dislocations. Polar dislocations accommodate incompatible strain gradients, and their long-range stress field induces anisotropic directional hardening. In contrast, randomly distributed dislocations ("statistical" dislocations) do not induce lattice curvature and produce a net internal stress field close to zero because their individual contributions statistically offset each other. In such a case, long-range interactions are screened by short-range interactions, and isotropic statistical forest hardening is

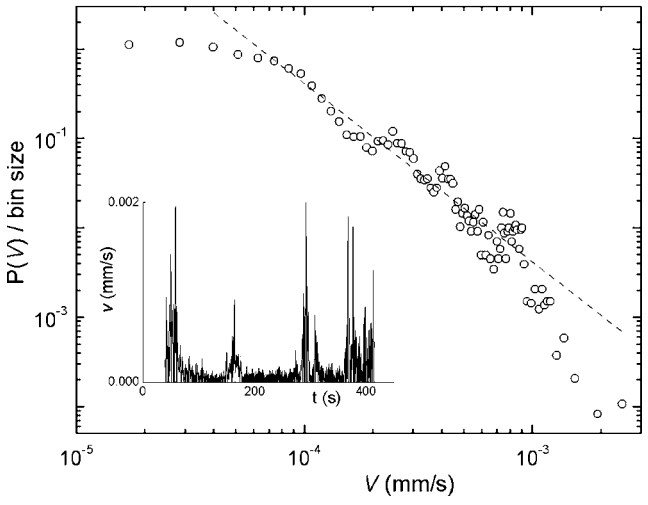

FIG. 5. Probability density function for peak values of the displacement velocity shown on Fig. 4. Peak values are normalized with respect to the averaged value over the time series. The dashed line indicates a power law trend with slope $\tau=2$.

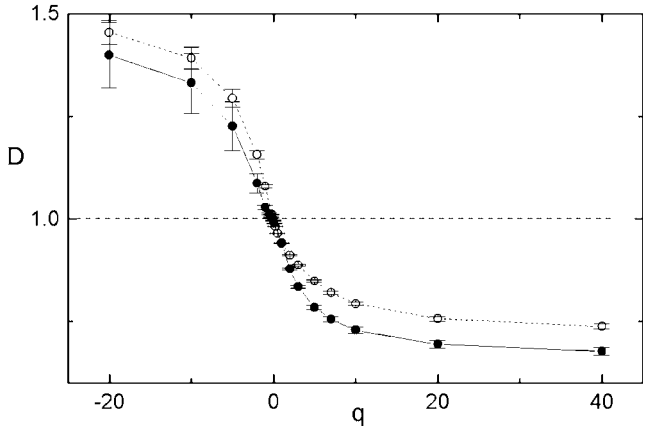

FIG. 6. Multifractal behavior of the velocity signals from high-resolution extensometry in Cu single crystals. Examples of the generalized dimension spectrum $D(q)$ for the local displacement velocity signal. Dark symbols: initial strain rate of 5×10^{-3} s^{-1}; light symbols: initial strain rate of 5×10^{-4} s^{-1} (signal shown in Fig. 4). The existence of a multifractal spectrum reveals a self-similar temporal structure of the signal, with an extended set of scaling exponents. The error bars were determined as least-squares estimates of the standard deviation of the slopes of the scaling dependences. For comparison, the dashed line corresponds to uniform (constant, periodic, or random) behavior [$\forall q$, $D(q)=1$]. A single fractal with fractal dimension D_f would correspond to a horizontal line with $\forall q$, $D(q)=D_f$. The spectra for other sections are very similar to those on display, an evidence of the robustness of temporal correlations.

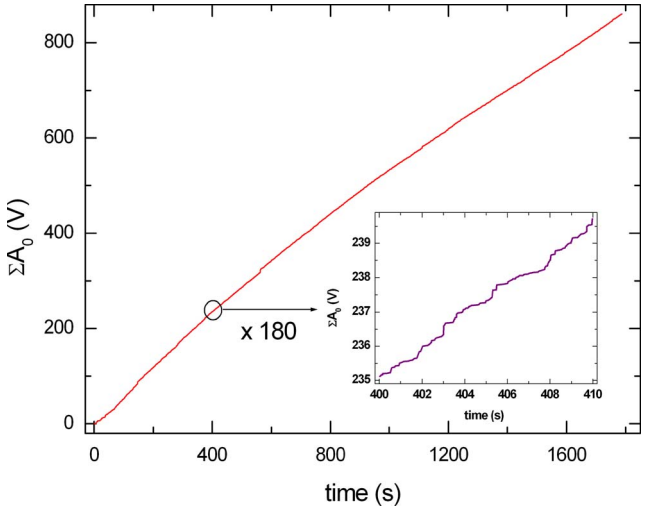

FIG. 7. (Color online) Compression creep experiment performed on an ice single crystals ($T=-10$ °C; and applied stress of 0.87 MPa). AE amplitudes cumulated from the onset of loading, ΣA_0, as a function of creep time. ΣA_0 is a proxy of the total strain and its time evolution appears smooth at the scale of the entire test (main graph), although a staircaselike curve is observed when one focuses over a small time window (inset). This smoothing of the curve towards large time scales is the result of truncated distributions of dislocation avalanche sizes. This figure is very similar to the electromagnetic emission accompanying plastic deformation of ionic crystals that appears smooth at large time scale and staircaselike at small time scale (Ref. 33).

observed. Driven, in particular, by their long-range stress field, polar dislocations rearrange by transport (collective motion) through the lattice. An example is the double cross slip of screw dislocations, which spreads dislocation activity from one glide plane to the next one.[26,27] The subsequent development of "slip bands," a well-studied phenomenon,[10,28] suggests a strongly anisotropic character for dislocations avalanches, which should spread over lamellar structures with a fractal dimension D significantly smaller than 3. This lamellar character of dislocation activity is also recovered in 3D discrete dislocation dynamics simulations.[8] It is also worth noting that fractal geometry of strain avalanches with $D\approx1.6$ was obtained in recent 3D molecular dynamics simulations of the plasticity of amorphous solids.[29] In this case, the anisotropy of avalanche spreading[30] cannot arise from the planar motion of dislocations over slip planes, but results only from internal stress interactions from localized events. On the other hand, dislocation avalanches are brief dynamic events,[7] but they interact over larger time scales through long-range elastic stress redistribution (although a possible role of anelastic relaxation of dislocations cannot be excluded). Hence, the observed scale-free pattern of global plastic activity[6] is likely to reflect the collective motion of these lamellar dislocation ensembles, more than the anisotropy of individual avalanche spreading.

In such a scale-free context, the smoothness of macroscopic strain curves seems paradoxical. Indeed, if the macroscopic strain ε_M is assumed to result from the cumulative effect of N strain increments ε distributed according to a Levy distribution of parameter $\beta\leqslant1$ [i.e., $P(\varepsilon)\sim\varepsilon^{-(1+\beta)}$, with $\varepsilon\rightarrow+\infty$], the rare (and extreme) events should dominate the global behavior ($\varepsilon_M=\Sigma_N\varepsilon\sim\varepsilon_{\max}$) (Ref. 31) and be detectable on macroscopic deformation curves whatever the strain gauge resolution. With $\beta=\tau-1\approx1$ [distributions of strain increments from micron-size samples give τ values slightly lower than 2, i.e., $\beta<1$ (Ref. 11)], we are here in this situation. However, if we stack AE amplitudes (i.e., ε) over a test (Fig. 7) or plot the overall displacement vs time (Fig. 3), we still obtain smooth curves at large scales. Thus, limiting factors to long-range correlations induced by internal stresses and dislocation transport must exist, and the distributions of avalanches must be truncated at large scales. This truncation is seen in the amplitude of velocity bursts in Cu single crystals (Fig. 5). Analytically, it is expressed as $P(\varepsilon)\sim\varepsilon^{-\tau}f(\varepsilon/\varepsilon_c)$, where ε_c is an avalanche characteristic size and $f(x)$ a cutoff function rapidly decaying toward large x. For AE amplitude distributions obtained in ice or metallic single crystals, it is too weak to be noticed on probability density distributions but is detectable on rank ordering statistics that emphasize the distribution tail [Fig. 1(b)].

Three limiting effects may be called for to explain such a cutoff: (i) a forest-hardening effect,[10,15] (ii) an elastic unloading effect, and (iii) a finite size effect due to the sample dimensions. (i) In the multislip conditions of stage II hardening, dislocations on various slip systems produce a more or less isotropic forest hardening. However, the absence of evolution in the avalanche distribution in hcp metals as the hardening rate θ jumps to higher values from stage I to stage II (Fig. 1) renders the forest-hardening hypothesis unlikely.

The fact that, for a given amplitude A, the average duration of events does not decrease when hardening increases further supports this view. Indeed, the coefficient α of relation (4) can be estimated from the $\Delta t \sim (1/\alpha)\log(A_0)$ relationship (averaging over many events of the same amplitude). In a previous work, α was found to increase (i.e., durations decrease) with increasing temperature, as the result of phonon drag, and with *kinematic* hardening in ice polycrystals.[7] In the experiments performed on metallic single crystals for the present work, we never observed any significant increase of α with increasing *isotropic* (or forest) hardening. The interpretation might be that, indeed isotropic hardening opposes locally the spreading of large avalanches, but that doing so, it favors displacement (transport) of dislocation activity to adjacent locations, not an overall cutoff. In addition, the truncation of slip step rank-ordering statistics observed in compression tests on ice single crystals (Fig. 1) and Ni microcrystals during stage I cannot originate in forest hardening, as the latter is negligible in single-slip conditions.[11] In multislip conditions, one might also conjecture that the formation of dislocation walls or cell boundaries would hinder the propagation of dislocation avalanches, as grain boundaries do.[13] This is again inconsistent with our results (absence of changes in the avalanche distribution or damping). The unstable, transient character of these features[32] might explain why they do not curb intermittency.

Under controlled displacement conditions, elastic unloading (ii) lowers the effective stress acting on all dislocations in the sample in proportion to the strain carried by the avalanche, and therefore, it has a cutoff effect. However, no such effect occurs in stress controlled experiments (e.g., creep tests) or in the mixed boundary conditions imposed on Ni microcrystals.[11] In such cases, the finite size of the sample (iii) should therefore play a role.

As for any dynamical system close to criticality, finite size must have effects on the development of the largest events (here, dislocation avalanches). Indeed, any critical behavior implies the divergence of the correlation length and is therefore necessarily affected by the finite dimensions of the system. In the present case, finite size can impinge on the avalanche initiation: the total dislocation length involved at the onset of the avalanche cannot be larger than the dislocation length that can be mobilized within the system. The propagation of avalanches can be affected as well, with free surfaces playing the role of dislocation sinks. The combination of these two effects sets limitations on the volume strained by the avalanche, $S \times b$ (where S is the area swept by all the dislocations involved in the avalanche and b the Burgers vector), and consequently, on the strain increment ε.

If the spreading of dislocation avalanches was dense and isotropic, a finite size effect would be felt for an avalanche size corresponding to a strained volume $S \times b$ scaling as the sample volume. More precisely, the strained volume would scale as d^3, where d is the characteristic dimension of the sample, and the cutoff strain increment ε_c would be independent of the sample size. However, dense and isotropic spreading of dislocation avalanches is incompatible with the development of slip bands, which supports instead the notion of dislocation avalanches spreading over lamellar structures characterized by a fractal dimension D significantly smaller than 3 (see above). Hence, the cutoff strained volume should scale as d^D instead of d^3 and the cutoff strain increment ε_c should scale as d^{D-3}. Therefore, it decreases with increasing sample size, which explains the smoothness of macroscopic deformation curves. In contrast, fluctuations of plastic activity are inescapable in submillimetric structures, with possible consequences in terms of formability.[8]

According to this scenario, the critical dynamics of intermittent plasticity is limited at large scales by the smallest sample dimension, as long as "extrinsic" obstacles to dislocation motion such as grain boundaries or precipitates do not confine avalanche propagation to small volumes of material,[13,14] or as long as an elastic unloading effect does not strengthen the truncation. This finite size effect is enhanced by the lamellar character of dislocation avalanches, which prohibits very large, macroscopically detectable strain bursts. This interpretation could explain why intermittency and scaling, although ubiquitous, are not perceived at macroscopic length scales and were essentially ignored so far in the modeling of plastic deformation.

ACKNOWLEDGMENTS

P.D. and F.C. acknowledge a support from the Ministry of Education of the Czech Republic (Research Plan MSM 0021620834) and from the Czech Grant Agency (Grant No. 103/06/0708). T.L. is grateful for the support of Centre National de la Recherche Scientifique through Grant No. DNE/1022. We thank H. Neuhäuser and Y. I. Chumlyakov for providing metallic single crystals, A.J. Beaudoin for stimulating discussions, as well as an anonymous reviewer for fruitful comments.

*weiss@lgge.obs.ujf-grenoble.fr

[1] L. P. Kubin, C. Fressengeas, and G. Ananthakrishna, in *Dislocations in Solids*, edited by F. R. N. Nabarro and M. S. Duesbery (Elsevier, Amsterdam, 2002).
[2] R. Becker and E. Orowan, Z. Phys. **79**, 566 (1932).
[3] J. Weiss and J. R. Grasso, J. Phys. Chem. **101**, 6113 (1997).
[4] M. C. Miguel, A. Vespignani, S. Zapperi, J. Weiss, and J. R. Grasso, Nature (London) **410**, 667 (2001).
[5] J. Weiss and M.-C. Miguel, Mater. Sci. Eng., A **387-389C** (2004).
[6] J. Weiss and D. Marsan, Science **299**, 89 (2003).
[7] T. Richeton, J. Weiss, and F. Louchet, Acta Mater. **53**, 4463 (2005).
[8] F. Csikor, C. Motz, D. Weygand, M. Zaiser, and S. Zapperi, Science **318**, 251 (2007).
[9] M. Koslowski, R. LeSar, and R. Thomson, Phys. Rev. Lett. **93**, 125502 (2004).
[10] M. Zaiser, Adv. Phys. **55**, 185 (2006).
[11] D. M. Dimiduk, C. Woodward, R. LeSar, and M. D. Uchic, Sci-

ence **312**, 1188 (2006).
[12] J. P. Sethna, K. A. Dahmen, and C. R. Myers, Nature (London) **410**, 242 (2001).
[13] T. Richeton, J. Weiss, and F. Louchet, Nat. Mater. **4**, 465 (2005).
[14] J. Weiss and F. Louchet, Scr. Mater. **54**, 747 (2006).
[15] M. C. Miguel and S. Zapperi, Science **312**, 1151 (2006).
[16] D. Rouby, P. Fleischman, and C. Duvergier, Philos. Mag. A **47**, 671 (1983).
[17] P. Bak, C. Tang, and K. Wiesenfeld, Phys. Rev. Lett. **59**, 381 (1987).
[18] F. Omori, J. Coll. Sci., Imp. Univ. Tokyo **7**, 111 (1894).
[19] P. Pirouz, in *Twinning in Advanced Materials*, edited by M. H. Yoo and M. Wuttig (The Minerals, Metals & Materials Society, Pittsburgh, 1994), p. 275.
[20] T. Richeton, P. Dobron, F. Chmelik, J. Weiss, and F. Louchet, Mater. Sci. Eng., A **424**, 190 (2006).
[21] N. I. Tymiak, A. Daugela, T. J. Wyrobek, and O. L. Warren, Acta Mater. **52**, 553 (2004).
[22] T. Imanaka, K. Sano, and M. Shimizu, Cryst. Lattice Defects **4**, 57 (1973).
[23] M. S. Bharathi, M. Lebyodkin, G. Ananthakrishna, C. Fressengeas, and L. P. Kubin, Phys. Rev. Lett. **87**, 165508 (2001).
[24] T. C. Halsey, M. H. Jensen, L. P. Kadanoff, I. Procaccia, and B. I. Shraiman, Phys. Rev. A **33**, 1141 (1986).
[25] M. A. Lebyodkin and T. A. Lebedkina, Phys. Rev. E **73**, 036114 (2006).
[26] M. Montagnat, J. Weiss, P. Duval, H. Brunjail, P. Bastie, and J. Gil Sevillano, Philos. Mag. **86**, 4259 (2006).
[27] O. Nittono, Jpn. J. Appl. Phys. **10**, 188 (1971).
[28] H. Neuhauser, in *Dislocations in Solids*, edited by F. R. N. Nabarro (North-Holland, Amsterdam, 1983), p. 319.
[29] N. P. Bailey, J. Schiotz, A. Lemaître, and K. W. Jacobsen, Phys. Rev. Lett. **98**, 095501 (2007).
[30] J. C. Baret, D. Vandembroucq, and S. Roux, Phys. Rev. Lett. **89**, 195506 (2002).
[31] D. Sornette, *Critical Phenomena in Natural Sciences* (Springer, Berlin, 2000).
[32] B. Jakobsen, H. F. Poulsen, U. Lienert, J. Almer, S. D. Shastri, H. O. Sorensen, C. Gundlach, and W. Pantleon, Science **312**, 889 (2006).
[33] Y. I. Golovin, M. A. Lebyodkin, A. A. Shibkov, M. A. Zheltov, V. V. Skvortsov, and R. Y. Koltsov, in *Fourth International Conference on Single Crystal Growth and Heat and Mass Transfer*, edited by V. P. Ginkin (Obninsk, Russia, 2001), Vol. 2, p. 543.